

PENTEC ORGAN SYSTEM REVIEW

Risk of Cerebrovascular Events Among Childhood and Adolescent Patients Receiving Cranial Radiation Therapy: A PENTEC Normal Tissue Outcomes Comprehensive Review



Jonathan F. Waxer, MD,^{*} Kenneth Wong, MD,[†] Arezoo Modiri, PhD,[‡] Anne-Marie Charpentier, MD,[§] Vitali Moiseenko, PhD,^{||} Cécile M. Ronckers, PhD,[¶] Phillip J. Taddei, PhD,^{#,***} Louis S. Constine, MD,^{††} Grant Sprow, BS,^{‡‡} Benita Tamrazi, MD,^{§§} Shannon MacDonald, MD,^{|||} and Arthur J. Olch, PhD[‡]

^{*}Department of Radiation Oncology, Southern California Permanente Medical Group, Los Angeles, California; [†]Radiation Oncology Program, Children's Hospital Los Angeles/Keck School of Medicine of the University of Southern California, Los Angeles, California; [‡]Department of Radiation Oncology, University of Maryland School of Medicine, Baltimore, Maryland; [§]Department of Radiation Oncology, Center Hospitalier de l'Université de Montréal, Montréal, QC, Canada; ^{||}Department of Radiation Medicine and Applied Science, University of California San Diego, La Jolla, California; [¶]Department of Pediatric Oncology, Princess Maxima Center for Pediatric Oncology, Utrecht, Netherlands; [#]Department of Radiation Oncology, Mayo Clinic, Rochester, Minnesota; ^{***}Department of Radiation Oncology, University of Washington School of Medicine, Seattle, Washington; ^{††}Department of Radiation Oncology and Pediatrics, University of Rochester Medical Center, Rochester, New York; ^{‡‡}Albert Einstein College of Medicine, Bronx, New York; ^{§§}Department of Radiology, Children's Hospital Los Angeles/Keck School of Medicine of the University of Southern California, Los Angeles, California; and ^{|||}Department of Radiation Oncology, Massachusetts General Hospital, Harvard Medical School, Boston, Massachusetts

Received Mar 2, 2022; Accepted for publication Jun 21, 2022

Purpose: Radiation-induced cerebrovascular toxicity is a well-documented sequelae that can be both life-altering and potentially fatal. We performed a meta-analysis of the relevant literature to create practical models for predicting the risk of cerebral vasculopathy after cranial irradiation.

Methods and Materials: A literature search was performed for studies reporting pediatric radiation therapy (RT) associated cerebral vasculopathy. When available, we used individual patient RT doses delivered to the Circle of Willis (CW) or optic chiasm (as a surrogate), as reported or digitized from original publications, to formulate a dose-response. A logistic fit and a Normal Tissue Complication Probability (NTCP) model was developed to predict future risk of cerebrovascular toxicity and stroke, respectively. This NTCP risk was assessed as a function of prescribed dose.

Results: The search identified 766 abstracts, 5 of which were used for modeling. We identified 101 of 3989 pediatric patients who experienced at least one cerebrovascular toxicity: transient ischemic attack, stroke, moyamoya, or arteriopathy. For a range of shorter follow-ups, as specified in the original publications (approximate attained ages of 17 years), our logistic fit model predicted the incidence of any cerebrovascular toxicity as a function of dose to the CW, or surrogate structure: 0.2% at 30 Gy,

Corresponding author: Kenneth Wong, MD; E-mail: kewong@chla.usc.edu

Disclosure: A.M.: Varian Medical System and University of Maryland Cancer Center, grant funding; spatial functional mapping and dose sensitivity of branching structures, patent. C.R.: Dutch Cancer Society Grant funding (SKON/AMNC 2012-5507). A.J.O.: NIH, grant funding; Sun Nuclear and Radiological Imaging Technology, consulting fees.

Data Sharing Statement: Research data are stored in an institutional repository and will be shared upon request to the corresponding author.

Supplementary material associated with this article can be found in the online version at [doi:10.1016/j.ijrobp.2022.06.079](https://doi.org/10.1016/j.ijrobp.2022.06.079).

Acknowledgments—The authors thank the American Association of Physicists in Medicine for logistical support and the Pediatric Normal Tissue Effects in the Clinic Steering Committee for guidance and feedback on this project. We also thank Marjorie Jones for designing Figure 1A.

1.3% at 45 Gy, and 4.4% at 54 Gy. At an attained age of 35 years, our NTCP model predicted a stroke incidence of 0.9% to 1.3%, 1.8% to 2.7%, and 2.8% to 4.1%, respectively at prescribed doses of 30 Gy, 45 Gy, and 54 Gy (compared with a baseline risk of 0.2%-0.3%). At an attained age of 45 years, the predicted incidence of stroke was 2.1% to 4.2%, 4.5% to 8.6%, and 6.7% to 13.0%, respectively at prescribed doses of 30 Gy, 45 Gy, and 54 Gy (compared with a baseline risk of 0.5%-1.0%).

Conclusions: Risk of cerebrovascular toxicity continues to increase with longer follow-up. NTCP stroke predictions are very sensitive to model variables (baseline stroke risk and proportional stroke hazard), both of which found in the literature may be systematically erring on minimization of true risk. We hope this information will assist practitioners in counseling, screening, surveilling, and facilitating risk reduction of RT-related cerebrovascular late effects in this highly sensitive population. © 2022 Elsevier Inc. All rights reserved.

Introduction

Radiation therapy (RT) is critical in the management of many pediatric brain malignancies and with continuing advances in oncological care, including cancer diagnosis and treatment, the life expectancies of pediatric cancer survivors continue to increase. There are many known adverse effects of RT on the brain including atrophy, radiation necrosis, gliosis as well as other vascular specific adverse effects: telangiectasias, microhemorrhages, cavernous malformations, and large vessel vasculopathies. The risk of vascular ischemia, thrombosis, or hemorrhage secondary to direct or incidental exposure of the cerebrovasculature to ionizing radiation is well documented and can predispose survivors to complications that may affect duration and quality-of-life.¹⁻⁵ As RT techniques and target identification and delineation continue to improve, a detailed understanding of radiation dose-response effects to the Circle of Willis (CW) and major cerebral arteries is imperative to maximize the therapeutic ratio of brain irradiation, and reduce the incidence of RT-induced cerebrovascular complications. This systematic review from the Pediatric Normal Tissue Effects in the Clinic committee⁶ aims to describe the risk of cerebral vasculopathy in cancer survivors who were treated with RT to the brain as children. We performed a meta-analysis of the relevant literature to generate practical models that help predict the risk of cerebrovascular toxicity. We created logistic fit dose-response and Normal Tissue Complication Probability (NTCP) models specific to our vasculopathic end points.

Clinical significance

After leukemia, solid tumors of the central nervous system (CNS) comprise the second most common cancers in children. In the United States, nearly 5000 solid tumors of the CNS are diagnosed annually in patients under the age of 20 years,⁷ and is the leading cause of cancer death in this population.⁸ Definitive or adjuvant RT continues to play an important role in the management of CNS tumors.

Radiation-induced brain injury has been described in 3 phases: acute (days to weeks after RT), early-delayed (within 1-6 months post-RT), and late (greater than 6 months post-RT).⁹ Generally, acute and early-delayed injuries are

transient, reversible, resolve spontaneously, and carry a benign clinical course, although some may evolve into more serious damage. Late brain injury is often considered irreversible and progressive and can involve neurologically devastating complications due to cerebrovascular changes.

Radiation-induced cerebral vasculopathies include a range of structural vascular changes and ischemic or hemorrhagic events. Stroke is a neurologic emergency that is among the most life-altering and potentially fatal sequelae of CNS irradiation. Several studies have shown childhood cancer survivors, especially patients who received RT to the brain, to be at increased risk of isolated or recurrent ischemic or hemorrhagic stroke.¹⁰⁻¹⁵ Mueller et al, for example, noted an overall rate of first stroke as 625 per 100,000 person-years after cranial and/or cervical neck RT¹³; this rate is far higher than the previously estimated annual population incidence rate of stroke of 2.3 per 100,000 in children, and approximately 7 to 15 per 100,000 person-years in young adults.^{16,17}

Cerebral microbleeds (CMBs), also known as cerebral microhemorrhages, are small, perivascular, parenchymal lesions that can be observed incidentally or in the context of a specific pathology (eg, cerebral amyloid angiopathy) or treatment course (ie, radiation-induced).¹⁸ CMBs are diagnosed histopathologically with focal accumulations of hemosiderin-containing macrophages, but now increasingly detected radiographically on magnetic resonance imaging, especially with the advent of more sensitive techniques (ie, gradient echo imaging and susceptibility-weighted imaging) to paramagnetic blood products causing signal loss due to susceptibility effects.^{19,20} CMBs are likely to occur within 3 years of completion of cranial RT and have been observed in up to 80% of pediatric brain tumor survivors.^{21,22} Risk factors for the development of CMBs include younger age at time of RT, higher maximum RT dose, and percent and absolute volume of brain exposed to ≥ 25 to 30 Gy.²¹⁻²⁴ CMBs are implicated in the subsequent development of worsening executive function, stroke, dementia, and small vessel ischemic disease, with greater incidence of these events with increasing attained age.^{23,25-27}

Estimates of cerebrovascular complications may be confounded in children with brain tumor predisposition syndromes, particularly neurofibromatosis type 1 (NF1), an autosomal dominant syndrome, which can also be associated with vascular abnormalities.²⁸ Children with NF1 have an increased risk of primary gliomas, such as low-grade

optic glioma, as well as a secondary malignant neoplasm. For example, a study from the Childhood Cancer Survivor Study cohort found 20-year cumulative incidences of secondary neoplasms in 7.3% versus 2.9% ($P = .003$) of NF1 and non-NF1 childhood cancer survivors, respectively, estimating a 2.4-fold higher risk of secondary neoplasms (95% confidence interval [CI], 1.3-4.3; $P = .005$) in NF1-affected individuals.²⁹ NF1 is also associated with greater risks of aneurysms and stenotic or ectatic cerebral vessels that subsequently increase the risk of ischemic and hemorrhagic stroke.³⁰⁻³³

Moyamoya disease, meaning “hazy” in Japanese, is a rare vasculopathy that is also associated with NF1. Moyamoya is characterized by stenosis or occlusion of intermediate and large-caliber cerebral arteries (Fig. 1) causing new angiogenesis and transdural anastomoses with the formation of abnormal complex vessel channels.³⁴ The small vessel collateralization produces a characteristic smoky appearance on angiography. Moyamoya disease tends to be progressive, and patients often suffer cognitive and neurologic decline due to repeated ischemic or hemorrhagic strokes.³⁵ Younger children less than 6 years of age at diagnosis have been observed to have more rapid progression and worse

prognosis than adults,³⁶ and in studies with long-term follow-up, progressive neurologic deficits and poor outcomes were reported in 50% to 66% of untreated patients.³⁷⁻³⁹ Besides NF1, moyamoya disease has also been associated with prior cranial RT.⁴⁰

Given the potentially devastating morbidity and mortality associated with RT-induced cerebral vasculopathy, there is significant reluctance to refer children for cranial RT, especially in certain patient populations such as those with NF1 who are also at an augmented risk of cerebral vasculopathy and RT-induced secondary malignancies. However, despite continued efforts to reduce the intensity of, or to omit, RT, to provide optimal disease control and survival, RT continues to play a pivotal role in many tumor types such as ependymoma, medulloblastoma, and germ cell tumors.^{41,42} Multiple retrospective series and case reports discuss the relationship between pediatric CNS irradiation and subsequent cerebral vasculopathy, but there are limited useful dose-response data. A better understanding of RT-induced cerebral vasculopathy, their typical time course to presentation, and RT doses associated with increased likelihood of adverse events, would help guide the oncology team in counseling, surveillance, and prevention.

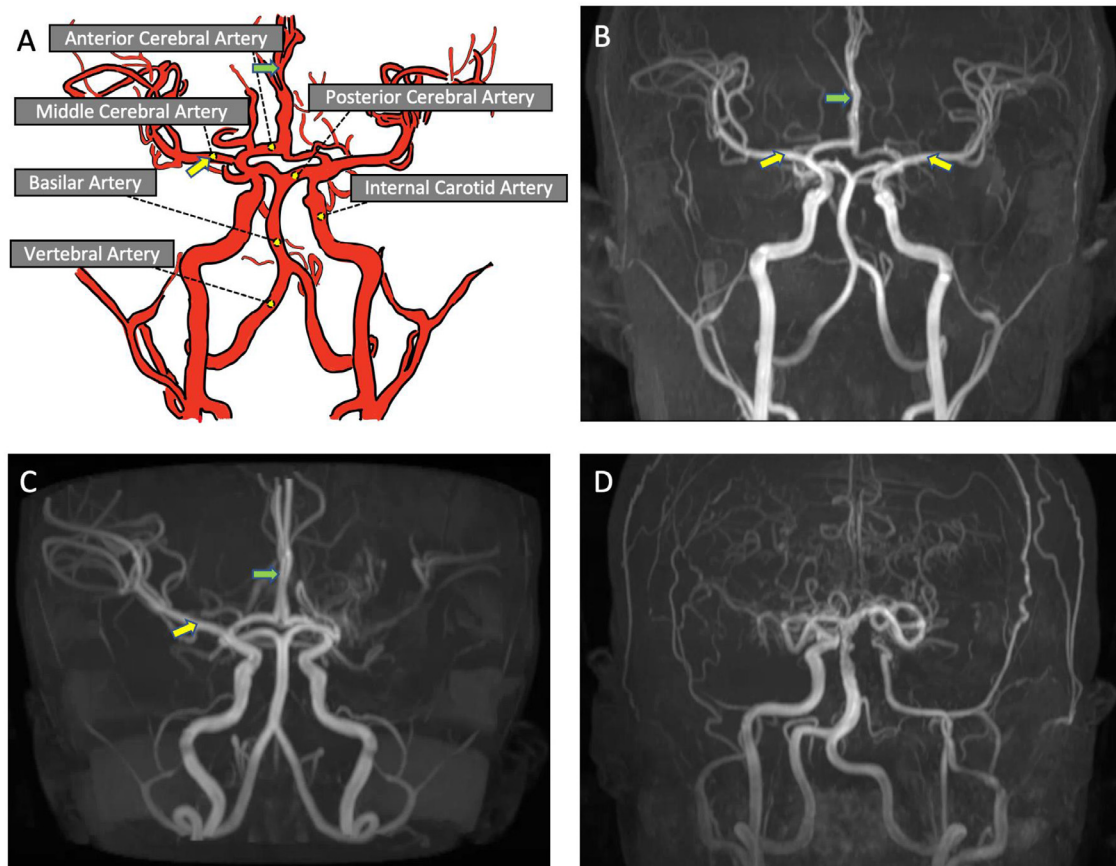


Fig. 1. Coronal view of Circle of Willis. A. Diagram of normal CW. B. Time-of-Flight MR Angiogram demonstrating normal flow. Middle cerebral arteries (yellow arrows) and anterior cerebral artery (green arrow). C. Unilateral Moyamoya demonstrating stenosis of the left middle cerebral artery. D. Moyamoya with bilateral stenosis of the supraclinoid portions of the internal cerebral arteries and non-visualization of the anterior and middle cerebral arteries.

End points and toxicity scoring

In this review, the end points we targeted were types of RT-induced cerebral arteriopathy or vasculopathy: ischemic or hemorrhagic events including transient ischemic attack (TIA), stroke, intracerebral or subdural hemorrhage, and moyamoya. We will henceforth reference these collective endpoints when describing “cerebrovascular toxicity.” Although the pathophysiology of the various endpoints differ, many of these cerebrovascular complications can result in life-altering consequences, and patients who had an ischemic TIA/stroke are at high risk of subsequent stroke.^{13,16,43,44} Therefore, discerning objective information on the dose-response relationship between RT dose to the CW or major cerebral arteries and any of our cerebrovascular end points was our objective. Ultimately, we did not include an exhaustive list of other RT-induced vasculopathic changes, such as cavernous malformations, telangiectasias, CMBs, or other preclinical radiographic arteriopathies seen on surveillance magnetic resonance angiography (MRA). The literature review methodology is summarized in the Review of Dose Volume Response Data and Risk Factors section.

The Common Terminology Criteria for Adverse Events (CTCAE) version 5.0 (<https://ctep.cancer.gov>) scores arterial thromboembolism, thromboembolic event, intracranial hemorrhage, cerebrovascular ischemia, TIA, and stroke based on imaging and clinical signs/symptoms. These toxicities are scored on a 5-point scale based upon the degree of deficit, radiographic visualization, hospitalization/intervention, or consequential death. Arterial thromboembolism and thromboembolic events are categorized under vascular disorders while intracranial hemorrhage, cerebrovascular ischemia, stroke, and TIA are specific to the CNS. In this review, many of the vasculopathic events occurred years after receiving RT to the brain, and most reports did not use a specific toxicity scoring/grading system, such as Radiation Therapy Oncology Group, European Organisation for Research and Treatment of Cancer, or CTCAE for cerebral vasculopathy. Rather, the diagnosis of vasculopathic events in many reports relied on imaging, histopathology, symptoms, or the need for invasive interventions. A large fraction of the events reported in the studies we analyzed would be considered clinically significant (eg, stroke), and we separated data available for different types of toxicity (eg, moyamoya, stroke) where possible. Due to the lack of clear grading of reported events we were unable to restrict our analysis to severe-only events, for example.

Anatomy and developmental dynamics

Vasculogenesis occurs around the fourth gestational week and the cerebrovasculature continues to mature and diversify in the first 3 or 4 years of postnatal life.^{45,46} Vascular endothelial growth factor and other angiogenic growth factors help promote vasculogenesis through the dynamic migration and extensive branching of the cerebrovasculature, and the CNS blood vessels continue to undergo vascular remodeling and endothelial cell recruitment of vascular

smooth muscle cells to form the mature functional CNS vasculature.⁴⁷⁻⁴⁹

Hypoxia appears to play a role in the evolution of RT-associated vascular injury, and age is a critical factor in the remodeling response to hypoxia. Tissue hypoxia stimulates multiple transcription factors that help promote the formation of angiogenic genes including vascular endothelial growth factor and erythropoietin which, in combination with other angiogenic factors, lead to changes in structure and function of cerebrovascular smooth muscle and the further development of new cerebral vessels.⁵⁰

Fetal cerebral arteries, relative to adults, have reduced overall contractility due to a smaller proportion of fully contractile cells. They constrict more slowly in response to rising arterial pressure and are less able in matching cerebral perfusion to local metabolic activity.⁵⁰ In the setting of chronic hypoxia, fetal cerebral arteries are less efficient at maintaining cerebrovascular homeostasis.

Younger patients are known to be more vulnerable to RT late effects, and small vessel microangiopathy is a well-studied complication of RT.^{51,52} Moyamoya and stroke have been more commonly observed in younger survivors of cranial RT,⁴⁰ although some discrepancies exist in the literature and contradict this observation.^{13,53}

Radiation-induced vascular injury is a complex molecular and pathophysiologic process which can affect blood vessels of all calibers with arteries and capillaries, relative to veins, being more sensitive to RT.⁵⁴⁻⁵⁸ In general, there is progressive endothelial loss that leads to increased vascular permeability with the disruption of the blood-brain barrier, vasogenic edema, and subsequent neural tissue hypoxia.⁵⁹ After initial endothelial loss, thrombi formation and hemorrhage develop, and ultimately vascular remodeling occurs leading to long-term morphologic changes, such as endothelial proliferation, basement membrane thickening, adventitial fibrosis, and vessel dilatation.⁶⁰ The result of these changes predispose survivors to a range of cerebral vasculopathic events due to cerebrovascular narrowing and fibrosis, new aberrant vasculature development and collateralization, changes in vascular flow and venous pressure, and vessel wall weakening, breakdown, and rupture.

Defining volumes: pediatric imaging issues

Whenever possible, we used the reported dose-volume histogram for the CW or the major cerebral arteries (see Fig. 1 for an example of these structures). However, only a few studies provided specific dose-volume data for those structures because the cerebrovasculature has rarely been routinely contoured, even though registration of diagnostic magnetic resonance imaging images with planning CT scans is routine for delineation of other structures, such as the optic chiasm or brain stem. Further, the cerebral vasculature can be challenging to identify on noncontrast CT simulation scans. MRA can enable more accurate delineation of the vascular structures, but dedicated vascular imaging is typically not performed clinically. Given the anatomic proximity and encircling of the optic chiasm by the CW, we used the

optic chiasm dose as a surrogate for the dose to the CW. Although smaller and unnamed vessels are certainly at risk of radiation damage which may lead to vasculopathy, there is a lack of data to model dose-response associations.

An atlas of the CW, large intracranial arteries, and suprasellar cistern (SC) were recently developed and internally validated and should be a useful tool for segmentation of the relevant structures.⁶¹ The authors also noted good agreement between maximum and mean doses to the CW when using SC as a surrogate (R^2 of 0.99 for both metrics). This level of agreement was consistent for all 3 tumor locations (central, lateral, and posterior fossa). When using the optic chiasm as a surrogate structure, Toussaint et al found good agreement for central ($R^2 = 0.97$) and lateral ($R^2 = 0.99$) groups, but the maximum dose to the CW was consistently underestimated for posterior fossa tumor locations ($R^2 = 0.76$). The R^2 values for the whole optic chiasm cohort reflected 0.95 and 0.83 for mean and maximum doses, respectively. To date, the SC has not been routinely contoured during treatment planning but could serve as a useful surrogate structure for future investigations, especially because the SC is easily delineated on CT-imaging (see Data Reporting Standards Specific to This Organ and Future Investigations sections).

Review of dose volume response data and risk factors

We developed a comprehensive list of search terms to identify all studies evaluating pediatric RT dose-volume effects on the risk of cerebral vasculopathy among survivors of childhood cancer of the brain. This systematic review was undertaken in accordance with the Preferred Reporting Items for Systematic Review and Meta-Analyses statement.⁶² PubMed and Cochrane Library searches of peer-reviewed manuscripts written in English and published before February 2019 were conducted. Appendix E1 provides further details of the search strategy, inherent biases, modeling details and data collection.

Six PENTEC investigators independently reviewed titles and abstracts and, subsequently, full texts of any article that any reviewer considered potentially eligible. Case reports lacking comparative control populations were excluded. For eligible studies, the same investigators independently extracted information on study design, source of data, population characteristics, and outcomes of interest using an electronic data extraction form. Eligibility assessment of the included studies, risk of bias assessment, and data extraction were performed independently and in duplicate.

Our search identified 766 unique references at title and abstract screening. After review by task force members, 7 studies (2 for stroke and one each for vasculopathy, arteriopathy, cerebrovascular mortality, moyamoya, and cavernous angioma) with potentially relevant information were selected. Cavernous angiomas were ultimately excluded due to their rare incidence, insufficient data points, and high likelihood of asymptomatic disease. Other relevant reports with repetitive data were excluded (ie, Haddy et al¹¹). Ultimately, 5 studies (5, 3, and 1 for TIA/stroke, moyamoya, and

arteriopathy, respectively) with pertinent information were herein analyzed. Of the original reports used in Table 1, Nordstrom et al¹⁴ was unique given the incorporation of regular surveillance MRAs in postcranial RT patients. This allowed them to observe imaging findings that met their criteria for radiographic arteriopathies before any clinical manifestations. Of their 10 observed arteriopathies, 5 had moyamoya, one had a stroke, and one had a TIA at time of last follow-up. Due to their consistent dose data prescribed to the CW and major cerebral arteries with narrow interquartile ranges in the arteriopathy and nonarteriopathy groups (54-55 and 54-55.8 Gy, respectively), we elected to graphically display their observations, but did not incorporate their preclinical end point into the logistic fit model (Fig. 2).

These 5 analyzed studies include 3989 survivors of solid childhood cancer under the age of 21 at initial treatment: 101 patients who experienced cerebrovascular toxicity and 132 total cerebrovascular events (95 stroke, 20 moyamoya, 10 radiographic arteriopathy, 7 TIA). Several patients experienced multiple or recurrent toxicities which were not counted as separate events in our analyses. Of these pediatric solid cancer survivors, 970 received no RT. The observed mean doses to the CW, major cerebral vessels, or surrogate optic chiasm, ranged from 0 to 79.5 Gy. Table 1 summarizes these studies.

Mathematical models

The follow-up period in the studies we analyzed was generally less than 14 years (relatively short) except for the article by El-Fayech,¹⁰ which included a median follow-up of 26 years. To provide more granular information, we segregated the data into 2 models predicting the risk of post-RT cerebral vasculopathy with varying lengths of follow-up: (1) the risk of cerebrovascular toxicity with shorter follow-up (Fig. 2, reflecting an attained age of approximately 17 years) and the risk of ischemic or hemorrhagic stroke on longer follow-up (Fig. 3, reflecting attained ages of 35 and 45 years). An attained age of approximately 17 years was chosen for the first model since patients were irradiated at an average age of 7 years, with approximately 10 years of follow-up. For the second model, El-Fayech et al¹⁰ specifically reported data at an attained age of 45 years, but we chose to also describe risk at an attained age of 35 years given the significant difference in baseline stroke incidence. The limitations of these models are discussed below under the Dose-Effect Associations section.

Estimating the risk of cerebrovascular toxicity

We attempted to create a dose-response model predicting the probability of post-RT cerebral vasculopathy. In the study by Omura et al,¹⁵ the mean dose to the CW and major cerebral arteries was significantly higher in patients who developed a cerebral vasculopathy compared with patients who did not experience a vasculopathic event (mean: 61 Gy vs 50 Gy; range, 54-79.5 Gy vs 19.5-66 Gy, $P < .05$). Dose-response is commonly assumed to follow a sigmoidal shape,

Table 1 Summary of key factors in the 5 analyzed studies

Study	End point	No. total pts	No. pts with vascular event	No. total events	Years of RT for cohort	Interval between RT and end point (y)	Type of reported dose/dose in region of interest (cGy)	Nature of dose data	Semi-objective dose accuracy Estimate (see text)
Omura et al ¹⁵ (1997)*	Vasculopathy	32	6	9 (4 stroke, 3 TIA, 2 moyamoya)	1980-1994	Median 5.2 (range 1.3-14)	Mean = 6100 Median = 5470 Range = 1950-7950	Prescribed in-field CW and major cerebral arteries	Within ~5%
Ullrich et al ⁴⁰ (2007)*	Moyamoya	345	12	24 (12 moyamoya, 9 stroke, 3 TIA)	1990-2000	Mean 3.9 (SD 1.8)	Mean (SD) = 5206 (635)	Calculated at optic chiasm or CW, unknown whether in TPS	Within ~5-10%
Mueller et al ¹³ (2013) [†]	Stroke	325	19	27 (6 recurrent, 1 multiply recurrent, 1 moyamoya)	1980-2009	Median 12 (IQR 5-18)	Mean (SD) = 5939 (1067)	Delivered dose to CW unknown, only prescribed tumor bed dose given	Within ~5% for whole brain, actual CW dose could be substantially different than prescribed dose for tumors not near the CW
El-Fayech et al ¹⁰ (2017)*, [†]	Stroke	3172	54	55 (39 ischemic, 16 hemorrhagic)	1942-1985	Median 26	Mean = 2200 for BTs, 1300 for NHL, 900 for Rb	Estimated CW dose based on geometric child phantom and chart review	Within ~5%-10%
Nordstrom et al ¹⁴ (2018)*	Arteriopathy	115	10	17 (10 arteriopathy, 5 moyamoya, 1 stroke, 1 TIA)	2011-2015	Mean 5.4 (SD 3.3)	Mean (SD) = 5454 (307) Median (IQR) = 5400 (5400-5500)	Prescribed in-field CW and involved arteries	Within ~5% for whole brain, ~5%-10% for focal

For El-Fayech et al, patients were placed into subgroups in the original report based on estimated doses to the CW: no RT or <1 Gy, 1 to 10 Gy, and >10 Gy dose.
Abbreviations: BT = brain tumor; CW = Circle of Willis; IQR = interquartile range; NHL = non-Hodgkin lymphoma; Rb = retinoblastoma; RT = radiation therapy; Rx = prescription; SD = standard deviation; TIA = transient ischemic attack; TPS = treatment planning software.
* Report incorporated into logistic fit model.
[†] Report incorporated into NTCP model.

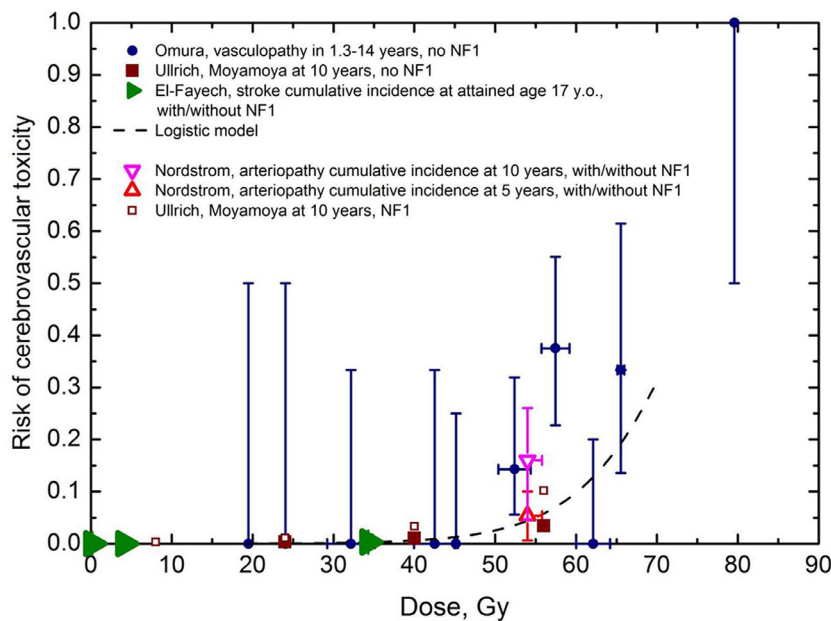


Fig. 2. Logistic fit model predicting the risk of cerebrovascular toxicity as specified in the original publications with RT dose. These risks are applicable to patients irradiated at an average age of 7 years, with approximately 10 years of follow-up, and an attained age of 17 years. Shown values were digitized from figures within original publications. The size of the symbol in our logistic model is reflective of the total number of patients in each report but is not proportional. In Omura, the horizontal error bars show standard deviations for doses for patients in each dose group, and the vertical error bars are 68% binomial confidence intervals calculated using the score method. For El-Fayech, patients were placed into subgroups in the original report based on estimated doses to the CW: No RT or <1 Gy, 1-10 Gy, and >10 Gy dose. In the data point from Nordstrom et al, horizontal error bars are an interquartile range, and vertical error bars are the incidence and 95% confidence intervals calculated by the Kaplan-Meier method. Nordstrom data are graphically displayed but were not incorporated into the logistic model. Patients with NF1 were removed from the logistic model unless the original report showed no statistically significant association between NF1 and subsequent cerebrovascular toxicity. The dashed line curve fit was truncated at 70 Gy reflecting the uncertainty in the model beyond the range of available data.

and popular modeling choices include logistic and probit.⁶³ We used a logistic model due to its easier interpretability that explains its common usage in similar previous studies (eg, HyTEC). A Cox model was not feasible due to lack of survival data in the listed studies, and actuarial incidences were derived from the presented figures with selected follow-up. The probability of cerebral vasculopathy was estimated by a logistic fit to individual patient data from our listed studies (Table 1). The probabilities of cerebrovascular toxicity were added to this 2-parameter logistic fit model (Fig. 2).

$$P(D) = 1/[1 + \exp[-4\gamma 50\lambda(D/D_{50} - 1)]]$$

Where:

- D is radiation dose to the CW, major cerebral arteries, or surrogate optic chiasm.
- $D_{50} = 75.6$ Gy (CI: 68.4-89.4) is a model parameter representing the dose at which the model projects 50% of patients to show complications.
- $\gamma_{50} = 2.69$ (2.05-3.60) is a model parameter representing the normalized normal tissue dose-response slope at D_{50} .

The best-fitting values were obtained using the maximum likelihood method, and the 95% confidence intervals were calculated using the profile-likelihood method.⁶³ Model parameter $D_{50} = 75.6$ Gy should not be interpreted literally as the dose truly causing 50% of patients to develop complications. It is a model parameter value obtained to achieve best fit to the observed data, as quantified using the maximum likelihood method. Projections to doses beyond the range of data availability are known to be model dependent. The data input into the model were the toxicity rates and corresponding dose metrics reported in each included study. Toxicity rates were converted to a proportionate number of binary outcomes according to the number of patients in each study.^{64,65} The maximum likelihood method accounts for the number of patients in each dose group. Therefore, the model is driven toward agreement with the data in the most “populated” dose range. The dashed line curve fit in Figure 2 was truncated at 70 Gy reflecting the uncertainty in the model beyond the range of available data.⁶³ The likelihood ratio test P value was < .001, demonstrating that the model statistically significantly improves on the null hypothesis assuming no dose-dependence.

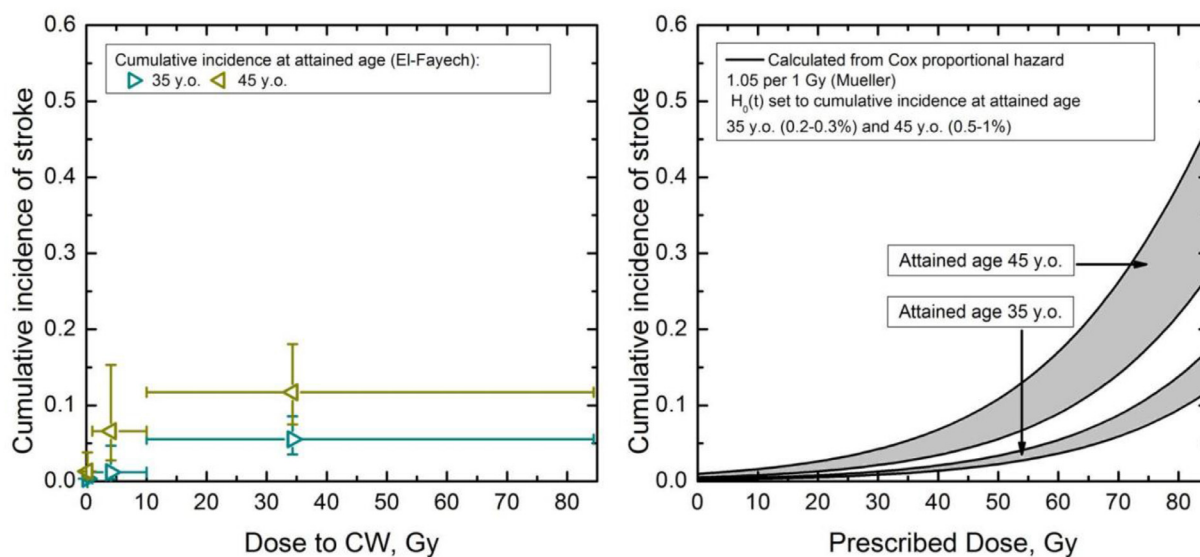


Fig. 3. Panel A (left) graphs the observed data from El-Fayech and the cumulative incidence of stroke at an attained age of 35 and 45 years. The x axis dose is the mean dose delivered to the Circle-of-Willis (CW). For El-Fayech, patients were placed into subgroups in the original report based on estimated doses to the CW: No RT or <1 Gy, 1-10 Gy, and >10 Gy dose. Triangular data points reflect the mean doses for the three dose bins. Horizontal error bars show the full range of dose within each group. 13 stroke events occurred among 386 patients with doses ranging 10-40 Gy and 16 stroke events occurred among 249 patients with doses >40 Gy. Vertical error bars are 95% confidence intervals as reported by El-Fayech. A fitted curve is not displayed due to the lack of adequate data. Panel B (right) is the normal tissue complication probability (NTCP) model for cumulative incidence of stroke at ages 35 and 45 versus radiotherapy dose using Mueller and El-Fayech studies, shown in the shaded regions between solid lines. These regions represent the variation in incidence for the indicated ranges of $H_0(t)$. The x axis dose is based on the prescribed dose to the primary tumor bed as reported in Mueller et al.'s study.

Estimating the risk of stroke

We extracted patient data from each selected study (Table 1) that observed post-RT stroke. Data from the listed studies and the baseline cumulative incidence of stroke in age-matched pediatric cancer patients who did not receive RT and in the general population, defined as $H_0(t)$, was used to create a proportional hazards NTCP model of stroke. This allowed us to investigate the probability of stroke corrected for actuarial incidence. Incidence of stroke is presented as a function of dose and attained age. Several studies included stroke as an end point but did not present their follow-up data as a function of time and thus could not be incorporated into the NTCP model. It was not possible to incorporate sex into dose-response fitting due to the lack of data. Another example is for moyamoya, where data shown separately for patients with versus without underlying NF (Fig. 4) demonstrated NF1 to be a significant parameter;⁴⁰ however, full proportional hazards data required for the NTCP model were not available.

The probability of future stroke was estimated using the formula:

$$\text{NTCP}_{\text{Cox}}(t, D) = 1 - e^{\Lambda(-H_0(t)e^{\Lambda\beta D})}$$

Where:

- t is an attained age at time of toxicity.
- D is radiation dose to the CW.

- $H_0(t)$ is the cumulative hazard function in absence of RT dose.
- β is the hazard ratio for dose.

For β we used values reported by Mueller et al, 2013.¹³ Mueller et al reported a 5% increase in "stroke hazard" defined as the percent increase risk in stroke hazard with each 1 Gy increase in RT dose (hazard ratio [HR] = 1.05; 95% CI, 1.01-1.09; $P = .02$). This proportional hazard from Mueller et al is based on prescribed dose to the primary tumor bed. For $H_0(t)$ we used a range of values reported by El-Fayech et al,¹⁰ the American Heart Association,⁴⁴ and the World Health Organization.⁶⁶ El-Fayech et al¹⁰ found the mean radiation dose to the CW as the key risk factor for ischemic and hemorrhagic strokes ($P < .0001$) and reported $H_0(t)$ for the general population: 0.22% at attained age of 35 years and 0.52% at attained age of 45 years.

Risk factors

A variety of therapeutic interventions (eg, surgery and systemic or intrathecal chemotherapies given concurrently or sequentially) can independently contribute to cerebral vasculopathies and can compound the effects of RT. Certain pediatric patients are at an increased baseline risk of stroke including those with genetic or congenital disorders (ie, NF1, thrombophilias, sickle cell disease, inborn errors of metabolism, congenital heart disease, etc). For example, Ulrich et al, 2007 noted the rate of moyamoya to be 3-fold in

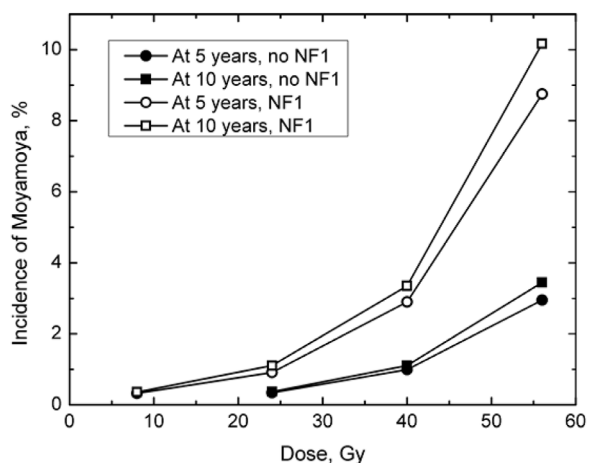


Fig. 4. Incidence of Moyamoya with respect to radiotherapy dose for patients with and without neurofibromatosis type 1 (NF1). The x axis represents mean dose to chiasm or circle of Willis. This graph is generated from Figure 2 in Ullrich et al. 2007.

patients with NF1 (HR = 3.07; 95% CI, 0.90-10.46; $P = .07$; Fig. 4).⁴⁰ Other clinical pathologies that have been associated with increased risk of stroke include malignancy, infection, autoimmune or inflammatory conditions, and trauma.⁶⁷⁻⁷¹

Generally, younger (vs older) ages at time of RT have been significantly associated with a higher risk of developing cerebrovascular toxicity,^{40,72,73} and as time elapses post-RT, the cumulative incidences of first stroke increases (eg, from 2% at 5 years to 17% at 20 years after RT). Additionally, these strokes occur in adolescence to young adulthood, ages for which the stroke risk in the general population is very low. In contradiction to many studies, Mueller et al¹³ noted an increased relative risk of stroke by 12% (1.12; 95% CI, 1.03-1.23; $P = .01$), and Campen et al⁵³ noted an increased relative risk of TIA/stroke by 13% (1.13; 95% CI, 1.02-1.25; $P = .018$) for every additional year of age at time of RT or cancer diagnosis, respectively.

Data suggest that women have a lesser risk for treatment-related stroke versus men.¹⁰ For example, El-Fayech et al¹⁰ noted cumulative incidences of stroke at age 50 of 10.4% (95% CI, 6.3%-16.8%) for men versus 3.4% (95% CI, 2.0%-

5.7%) for women. In an attempt to consider dose dependence, the excess relative risk of stroke per gray (ERR/Gy) was also higher in men (ERR/Gy = 0.39; 95% CI, 0.18-0.84) versus women (ERR/Gy = 0.11; 95% CI, 0.02-0.30). This was further reinforced ($P < .001$) when the analysis was restricted to ischemic strokes only, where the ERR/Gy was 0.68 (95% CI, 0.26-1.87) in men and 0.13 (95% CI, 0.01-0.53) in women. Nordstrom et al,¹⁴ however, noted higher risk of arteriopathy in females ($P = .038$). The present review was not large enough to consider the potential variation in risk based on chemotherapy, surgery, sex, or age.

**Dose-effect associations
Cerebrovascular toxicity**

Our logistic fit dose-response curve for cerebrovascular toxicity is dependent on RT dose to the CW/major cerebral arteries, or surrogate optic chiasm. For the range of follow-up given in the aforementioned studies (approximate attained ages of 17 years), the predicted incidence of cerebrovascular toxicity was 0.2% at 30 Gy, 1.3% at 45 Gy, and 4.4% at 54 Gy (Fig. 2).

Stroke

Our NTCP model predicted the risk of stroke with longer follow-up (attained ages of 35 and 45 years old) as a function of prescribed tumor bed dose (Fig. 3). The shaded regions show the ranges of expected cumulative incidences of stroke for attained ages of 35 and 45 years based on proportional hazards results. The listed projections are subject to uncertainties, in particular due to the proportional stroke hazard for prescribed dose to the primary tumor bed rather than dose to the CW and the associated $H_0(t)$. $H_0(t)$ was estimated to be between 0.2% to 0.3% at an attained age of 35 years, and 0.5% to 1.0% at an attained age of 45 years. NTCP model projections to zero dose are almost equal to baseline risk. Results are listed below and in Table 2.

- At an attained age of 35 years, the predicted incidence of stroke was 0.9% to 1.3% at 30 Gy, 1.8% to 2.7 % at 45 Gy, and 2.8% to 4.1% at 54 Gy.
- At an attained age of 45 years the predicted incidence of stroke was 2.1% to 4.2% at 30 Gy, 4.4% to 8.6% at 45 Gy, and 6.7% to 13.0% at 54 Gy.

Table 2 Risk of stroke after cranial RT

	$H_0(t)$, %	Risk of stroke after		
		30 Gy (%)	45 Gy (%)	54 Gy (%)
Attained age of 35 y	0.2	0.9	1.8	2.8
	0.3	1.3	2.7	4.1
Attained age of 45 y	0.5	2.1	4.4	6.7
	1.0	4.2	8.6	13.0

Listed percentiles are the suggested Normal Tissue Complication Probability risk of stroke at attained ages of 35 and 45 years of age with specified doses of radiation and baseline cumulative incidences of stroke. Stroke risk is based on the prescribed dose to the primary tumor bed as reported in Mueller et al.¹³
Abbreviations: $H_0(t)$ = cumulative hazard function in absence of cranial RT; RT = radiation therapy.

Overall, pediatric patients have a very low baseline risk of stroke, and, even after receiving higher nominal doses of RT, their risk of stroke remains fairly low until significant follow-up is achieved (ie, attained ages of 45 years). This is likely affected by the development of other lifestyle factors and comorbid conditions that precipitously increase baseline stroke risks. The risk of toxicity from all types of cerebrovascular events of course appears greater than stroke alone, even at a relatively young attained age, 4.4% at 54 Gy and an attained age of 17 years old versus up to 4.1% and an attained age of 35, respectively. Caution must be taken when comparing logistic and NTCP models due to the difference in follow-up, end point(s), and the uncertainty in received CW dose reported by Mueller et al (see Limitations section). We anticipate the need for future adjustments to these risk estimates with evolving data and improved surveillance imaging.

Van Dijk et al, 2016 performed a cohort study with similarly long-term follow-up evaluating the risk of symptomatic stroke in 1362 survivors of childhood cancer. They estimated the cumulative incidence of stroke by the age of 45 years as 10.0% (95% CI, 2.5%-17.0%) in patients who received cranial RT with a median EQD2 (equivalent dose in 2 Gy fractions) of 39.2 Gy (range, 22.3-76.6 Gy) in patients with stroke, and 26.3 Gy (10.8-247.5 Gy) in patients without stroke.⁷⁴ This estimate falls within our reported range of NTCP stroke risk at the same attained age of 45 years (Table 2). Ultimately, their data were not incorporated into our modeling efforts for several reasons. First, there is significant heterogeneity in patient cohort and treatment techniques. They reported incidence of stroke with cranial RT, supradiaphragmatic RT, or both, but do not show how this incidence varies as a function of dose and unexpectedly noted patients who received supradiaphragmatic RT to be at a higher risk of subsequent stroke, compared with cranial RT (HR 1.04 [1.02-1.05] vs 1.02 [1.01-1.03], respectively). A further limitation of the study is that prescribed dose, rather than dose to the region of interest has been used. Second, their reported RT doses for patients with and without a stroke event was unsuitable for secondary analysis in modeling dose-response due to a single reported median dose with broad EQD2 ranges (eg, 10.8-247.5 Gy for controls) that the median is likely unrepresentative of the dose for all patients. Additionally, their reported baseline stroke incidence was quite low at 0.1% (95% CI, 0%-0.4%) at an attained age of 45 years in childhood cancer survivors who did not receive cranial or supradiaphragmatic RT and seems to be based on a single stroke event.

Limitations

This analysis has all the limitations common to the pooling of data from retrospective studies. Our analysis and modeling were limited to the consideration of the most consistently reported variables in the selected studies, with variable lengths of follow-up, interstudy reporting approaches, etc. Further, we were unable to convert

prescribed doses into equivalent doses with 2 Gy per fraction because many investigations simply reported a nominal dose to the region of interest, rather than a dose/fractionation.

Several reports contained populations of patients with and without NF1. NF1 is a known risk factor of future cerebrovascular events, and therefore we did not include these patients in our modeling unless the original report showed no statistically significant association between NF1 and subsequent cerebrovascular toxicity. Overall, the total number of patients with NF1 was small (65/3989), and most of these (56/65) developed no observed cerebrovascular toxicity. Therefore, the effect of NF1 could not be assessed in our models due to lack of sufficient data, although we expect NF patients to be at an augmented risk of developing cerebrovascular toxicity compared with the estimates reported here. Our NTCP model projections are very sensitive to $H_0(t)$ and the accuracy of RT dose estimates, as discussed below.

Baseline stroke risk for the general population and nonirradiated pediatric cancer survivors

Consistent baseline stroke rates are challenging to identify because rates vary by age range studied, population of interest, and definition used. Data published by the World Health Organization suggest the baseline cumulative incidence of stroke in the Americas is 0.3% and 1.7% at attained aged 30 to 44 and 45 to 59 years, respectively.⁶⁶ The American Heart Association reported stroke prevalence rates of 0.5% and 2.0% at age ranges of 20 to 39 and 40 to 59 years, respectively.⁴⁴ Although technically different, cumulative incidence of stroke by an attained age of 45 and the prevalence of stroke in an individual at the age of 45 should yield similar rates. We used values that were previously published by El-Fayech¹⁰ for their study population, suggesting a baseline cumulative incidence of stroke of 0.22% at an attained age of 35 years and 0.52% at an attained age of 45 years in the general population. The incidence of stroke was very similar in the general population and pediatric cancer survivors who received either no RT or <1 Gy, until the age of 45. We opted to use a range of values for $H_0(t)$, 0.2% to 0.3% at an attained age of 35 years and 0.5% to 1.0% at an attained age of 45 years, as a best estimate for the baseline cumulative incidence of stroke in pediatric cancer survivors and the general population. Modest changes to the baseline risk could meaningfully affect the apparent excess risk and thus the NTCP modeling. NTCP risk estimates will improve as more extensive data becomes available (especially as presented with our suggested recommendations; see Data Reporting Standards Specific to This Organ section).

Accuracy of RT dose estimates and the proportional stroke hazard

Dose is clearly a dominant factor in the risk of vascular injury.^{4,10,15} The task force medical physicist performed a somewhat subjective dose accuracy evaluation for each investigation analyzed for dose-response modeling that

included a categorization of the reported doses as well as an estimate, when possible, of the accuracy of those doses (Table 1). The main limitation in our systematic review was in some of the reported doses to the CW. Specifically, the uncertainties in CW doses reported from some studies were unclear and difficult to estimate. We examined these data further and, in some cases, contacted the original authors for more details. If we could not establish their uncertainties with confidence, we removed them from our model. One investigation reported prescribed mean or median doses to the optic chiasm, and some investigations reported only prescribed dose rather than organ of interest dose (ie, CW or major cerebral arteries). The dose accuracy to the CW for the articles used in our analysis was generally 5% to 10% (Table 1) except for the Mueller article, which did not state the dose to the CW but instead to the primary tumor bed which could be distant from the CW, and thus the dose accuracy to the CW is potentially large. For our NTCP model, the doses used were the prescribed doses and not the actual CW dose. This is of particular concern because many primary targets in children are in regions in the brain distant from the CW. A common scenario is for patients to receive wide-field RT (eg, whole brain or craniospinal) to 36 Gy, followed by a posterior fossa boost. In these cases, ascribing the observed excess stroke risk to the higher (eg, posterior fossa) dose would tend to make our NTCP models underestimate the risk, perhaps significantly so, and is a major limitation to our NTCP model. The Omura¹⁵ and Nordstrom¹⁴ article similarly assigned the prescribed dose to the organ of interest, which presents an unknown degree of error in dose-response. For the El-Fayech¹⁰ article, which has the largest number of patients and cases, the authors calculated the dose to the CW using a pediatric phantom with 5% to 10% dosimetric accuracy. Unlike the other articles used in our analysis, this article used dose binning with large dose bin sizes which may reduce the accuracy of the dose-response results.

Clinical effect

Despite the known risks associated with RT to children's brain, RT remains an essential component in the definitive management of many childhood brain tumors. When treating this vulnerable population, potential morbidities should be considered and discussed with the family and the treating team. Patients may benefit from monitoring and early detection of late effects; early intervention may mitigate some of the known risks.

Toxicity scoring recommendations

The following methods for toxicity scoring are recommended:

- Use CTCAE version 5.0 criteria for grading toxicity for arterial thromboembolism, thromboembolic event, intracranial hemorrhage, cerebrovascular ischemia, TIA, and stroke based on imaging and clinical description of symptoms. These toxicities are scored on a 5-point scale based on the degree or duration of deficit, if

visualized radiographically, whether hospitalization or intervention was indicated, or if death resulted.

Data reporting standards specific to this organ

Systematic dosimetric analyses based on published data of RT-induced cerebral vasculopathies are limited for several reasons, for example: (1) minimal radiation dose or volume information exist due to lack of baseline vascular imaging and lack of delineation during RT planning, (2) many cerebrovascular toxicities occur years after treatment and these adverse events are not routinely graded, and (3) pooling of incomplete data from combined large inhomogenous patient cohorts. Some pooled reports had repetitive patient data, which had to be carefully analyzed for redundancies and excluded from modeling efforts. Consequently, it is vital that published data sets conform to rigorous reporting standards to facilitate data pooling. Thus, we propose reporting the following information in future studies:

- Patient sex and race
- Patient-specific genetic susceptibilities and/or relevant PMH (ie, NF1, previous stroke)
- Clinical indication for RT (ie, malignant neoplasm, benign tumor, arteriovenous malformation)
- Age when treated with RT, frequency of follow-up, attained age at time of toxicity, and age at last follow-up
- Prescribed RT dose and dose/fractionation
- RT modality (photons, protons, other charged particles)
- Dosimetric data for patients, both those with and without toxicity
 - Prescription dose, organ radiation exposure, described by relevant normal organ dose-volume histograms with mean and maximum doses, including the dose to a small volume (ie, 0.03 cc) rather than a point dose maximum.
 - Include brain and vascular substructures such as the optic chiasm, CW, and SC (see atlas referenced by Toussaint). The CW can be segmented as a region rather than each separate vessel, and the SC has been an internally validated surrogate structure for mean and maximum CW dose.⁶¹
- Chemotherapy use (if yes, timing with respect to RT and agents used)
- Number of studied patients; both with and without toxicity (both overt and subclinical)
 - Toxicity end points
 - Description of the toxicity end point including how it is measured
 - Description of which toxicity scoring system was used
 - Grade or severity of end point in patients

Future investigations

Additional studies are needed to better understand:

- 1) What are the factors affecting the risk of RT-induced cerebral vasculopathies? Including:

- a) Pre-RT patient-related factors (eg, age, concurrent illnesses, genetic)
- b) Tumor-related factors (eg, tumor type, size, location)
- c) Treatment-related factors, eg:
 - i) RT details: dose, volume, fractionation, modality
 - 1) The association of both clinical and subclinical vasculopathy with increased RT dose is increasingly clear. It has been theorized that modalities with increased dose heterogeneity (eg, passive scattering proton beam therapy) may predispose to vascular injury given a higher risk of dose “hotspots.”⁷⁵ Further, the higher radiobiological effectiveness of proton beam therapy relative to photons may also contribute to an increased risk of underlying vascular injuries.⁷⁶ Further data are needed to better understand the effects of treatment modality in this regard.
 - ii) Other: chemotherapy, surgery
 - d) Post-RT patient-related factors (eg, later development of diabetes, hypertension, or metabolic syndrome that may also increase stroke risk)
 - i) Knowing which children are at greatest risk may help to personalize treatment recommendations, or post-RT screening regimens that are directed toward characterizing the neurovasculature.
- 2) What are the factors that affect the kinetics of toxicity, both latency time to toxicity and its clinical course (eg, plateau, progress, or recovery)?
 - a) This is critical because, for example, El-Fayech et al¹⁰ noted that even moderate RT doses to the CW (range, 1-10 Gy; mean, 4 Gy) increased the risk of stroke by a factor of 5.0 (95% CI, 1.4-17.4), and the risk coefficients increased with longer follow-up times. Further data may help inform and guide future standardization of follow-up evaluations for surveillance.
- 3) How can we better exploit imaging to study this issue?
 - a) Can we adopt standard pre-RT imaging approaches to facilitate delineation (and, if possible, sparing of these structures) during planning?
 - i) We recognize that delineation of the vasculature is tedious and impractical in the routine clinical setting. A specific RT consensus contouring guideline of the CW and major cerebral arteries would be helpful for practitioners to better delineate and avoid these sensitive substructures. AI-based auto-segmentation of the region or of the vessels and use of atlases may be useful, as they become increasingly available. Otherwise, at a minimum, we recommend routine delineation of surrogate structures such as the optic chiasm and SC.
 - b) Can we adopt standard post-RT imaging to monitor for subclinical injury? For example, Nordstrom et al¹⁴ performed annual posttreatment surveillance MRA imaging that revealed evidence of radiographic arteriopathies before clinical toxicity events occurred.

- i) Ideally, all patients would have baseline assessment of their cerebrovasculature (eg, with MRA before RT) to document the effect of the surgery or the tumor itself on the cerebrovasculature. Then, patients would have repeat imaging at multiple time points after RT to determine changes, guide care and possible early interventions. However, accessibility to MRA can be limited and a baseline assessment can be challenging to obtain depending on the patient's postoperative status, the urgency to start adjuvant treatment, and cost-effectiveness issues.
- c) What is the association between asymptomatic (eg, grade 1) injury (eg, seen on MRA) and symptomatic injury?
- d) What is the effect of volume and location of irradiated cerebrovasculature (ie, anterior cerebral artery, middle cerebral artery, posterior cerebral artery, communicating arteries, basilar artery, etc)? Will specific regions/substructures of the cerebrovasculature be particularly sensitive to RT and be preferentially avoided? Will advanced RT techniques that reduce dose to cerebrovascular organs at risk decrease the incidence of late toxicities?

References

1. Armstrong GT, Stovall M, Robison LL. Long-term effects of radiation exposure among adult survivors of childhood cancer: Results from the childhood cancer survivor study. *Radiat Res* 2010;174:840–850.
2. Fullerton HJ, Stratton K, Mueller S, et al. Recurrent stroke in childhood cancer survivors. *Neurology* 2015;85:1056–1064.
3. Möller TR, Garwicz S, Barlow L, et al. Decreasing late mortality among five-year survivors of cancer in childhood and adolescence: A population-based study in the Nordic countries. *J Clin Oncol* 2001;19:3173–3181.
4. Mueller S, Fullerton HF, Stratton K, et al. Radiation, atherosclerotic risk factors, and stroke risk in survivors of pediatric cancer: A report from the childhood cancer survivor study. *Int J Radiat Oncol Biol Phys* 2013;86:649–655.
5. Reulen RC, Winter DL, Frobisher C, et al. Long-term cause-specific mortality among survivors of childhood cancer. *JAMA* 2010;304:172–179.
6. Constine LS, Olch AJ, Jackson A, et al. Pediatric Normal Tissue Effects in the Clinic (PENTEC): An international collaboration to assess normal tissue radiation dose-volume-response relationships for children with cancer. *Int J Radiat Oncol Biol Phys* 2024;119:316–320.
7. Ostrom QT, Gittleman H, Truitt G, et al. Cbtrus statistical report: Primary brain and other central nervous system tumors diagnosed in the United States in 2011–2015. *Neuro Oncol* 2018;20(Suppl 4):iv1–iv86.
8. Curtin SC, Minino AM, Anderson RN. Declines in cancer death rates among children and adolescents in the United States, 1999–2014. *NCHS Data Brief* 2016;1–8.
9. Tofilon PR, Fike JR. The radioresponse of the central nervous system: A dynamic process. *Radiat Res* 2000;153:357–370.
10. El-Fayech C, Haddy N, Allodji RS, et al. Cerebrovascular diseases in childhood cancer survivors: Role of the radiation dose to Willis circle arteries. *Int J Radiat Oncol Biol Phys* 2017;97:278–286.
11. Haddy N, Mousannif A, Tukenova M, et al. Relationship between the brain radiation dose for the treatment of childhood cancer and the risk of long-term cerebrovascular mortality. *Brain* 2011;134(Pt 5):1362–1372.

12. Mitchell WG, Fishman LS, Miller JH, et al. Stroke as a late sequela of cranial irradiation for childhood brain tumors. *J Child Neurol* 1991;6:128–133.
13. Mueller S, Sear K, Hills NK, et al. Risk of first and recurrent stroke in childhood cancer survivors treated with cranial and cervical radiation therapy. *Int J Radiat Oncol Biol Phys* 2013;86:643–648.
14. Nordstrom M, Felton E, Sear K, et al. Large vessel arteriopathy after cranial radiation therapy in pediatric brain tumor survivors. *J Child Neurol* 2018;33:359–366.
15. Omura M, Aida N, Sekido K, et al. Large intracranial vessel occlusive vasculopathy after radiation therapy in children: Clinical features and usefulness of magnetic resonance imaging. *Int J Radiat Oncol Biol Phys* 1997;38:241–249.
16. Fullerton HJ, Wu YW, Zhao S, et al. Risk of stroke in children: Ethnic and gender disparities. *Neurology* 2003;61:189–194.
17. Griffiths D, Sturm J. Epidemiology and etiology of young stroke. *Stroke Res Treat* 2011;2011 209370.
18. Haller S, Vernooij MW, Kuijper JPA, et al. Cerebral microbleeds: Imaging and clinical significance. *Radiology* 2018;287:11–28.
19. Cheng AL, Batool SB, McCreary CR, et al. Susceptibility-weighted imaging is more reliable than T2*-weighted gradient-recalled echo MRI for detecting microbleeds. *Stroke* 2013;44:2782–2786.
20. Vernooij MW, Ikram MA, Wielopolski PA, et al. Cerebral microbleeds: accelerated 3D T2*-weighted GRE MR imaging versus conventional 2D T2*-weighted GRE MR imaging for detection. *Radiology* 2008;248:272–277.
21. Kralik SF, Mereniuk TR, Grignon L, et al. Radiation-induced cerebral microbleeds in pediatric patients with brain tumors treated with proton radiation therapy. *Int J Radiat Oncol Biol Phys* 2018;102:1465–1471.
22. Passos J, Nzwalo H, Marques J, et al. Late cerebrovascular complications after radiotherapy for childhood primary central nervous system tumors. *Pediatr Neurol* 2015;53:211–215.
23. Roddy E, Sear K, Felton E, et al. Presence of cerebral microbleeds is associated with worse executive function in pediatric brain tumor survivors. *Neuro Oncol* 2016;18:1548–1558.
24. Tanino T, Kanasaki Y, Tahara T, et al. Radiation-induced microbleeds after cranial irradiation: Evaluation by phase-sensitive magnetic resonance imaging with 3.0 tesla. *Yonago Acta Med* 2013;56:7–12.
25. Charidimou A, Krishnan A, Werring DJ, et al. Cerebral microbleeds: A guide to detection and clinical relevance in different disease settings. *Neuroradiology* 2013;55:655–674.
26. Werring DJ, Gregoire SM, Cipolletti L. Cerebral microbleeds and vascular cognitive impairment. *J Neurol Sci* 2010;299:131–135.
27. Van der Flier WM, Cordonnier C. Microbleeds in vascular dementia: Clinical aspects. *Exp Gerontol* 2012;47:853–857.
28. Meulepas JM, Ronckers CM, Merks J, et al. Confounding of the association between radiation exposure from CT scans and risk of leukemia and brain tumors by cancer susceptibility syndromes. *J Radiol Prot* 2016;36:953–974.
29. Bhatia S, Chen Y, Wong FL, et al. Subsequent neoplasms after a primary tumor in individuals with neurofibromatosis type 1. *J Clin Oncol* 2019;37:3050–3058.
30. Kaas B, Huisman TA, Tekes A, et al. Spectrum and prevalence of vasculopathy in pediatric neurofibromatosis type 1. *J Child Neurol* 2013;28:561–569.
31. Koss M, Scott RM, Irons MB, et al. Moyamoya syndrome associated with neurofibromatosis type 1: Perioperative and long-term outcome after surgical revascularization. *J Neurosurg Pediatr* 2013;11:417–425.
32. Rea D, Brandsema JF, Armstrong D, et al. Cerebral arteriopathy in children with neurofibromatosis type 1. *Pediatrics* 2009;124:e476–e483.
33. Rosser TL, Vezina G, Packer RJ. Cerebrovascular abnormalities in a population of children with neurofibromatosis type 1. *Neurology* 2005;64:553–555.
34. Burke GM, Burke AM, Sherma AK, et al. Moyamoya disease: A summary. *Neurosurg Focus* 2009;26:E11.
35. Morioka M, Hamada J, Todaka T, et al. High-risk age for rebleeding in patients with hemorrhagic moyamoya disease: Long-term follow-up study. *Neurosurg* 2003;52:1049.
36. Kim SK, Seol HJ, Cho BK, et al. Moyamoya disease among young patients: Its aggressive clinical course and the role of active surgical treatment. *Neurosurg* 2004;54:840.
37. Choi JU, Kim DS, Kim EY, et al. Natural history of moyamoya disease: Comparison of activity of daily living in surgery and non surgery groups. *Clin Neurol Neurosurg* 1997;99(Suppl 2):S11.
38. Ezura M, Yoshimoto T, Fujiwara S, et al. Clinical and angiographic follow-up of childhood-onset moyamoya disease. *Childs Nerv Syst* 1995;11:591.
39. Kurokawa T, Tomita S, Ueda K, et al. Prognosis of occlusive disease of the Circle of Willis (moyamoya disease) in children. *Pediatr Neurol* 1985;1:274.
40. Ullrich NJ, Robertson R, Kinnamon DD, et al. Moyamoya following cranial irradiation for primary brain tumors in children. *Neurology* 2007;68:932–938.
41. Dhall G, O'Neil SH, Ji L, et al. Excellent outcome of young children with nodular desmoplastic medulloblastoma treated on "head start" III: A multi-institutional, prospective clinical trial. *Neuro Oncol* 2020;22:1862–1872.
42. Merchant TE, Bendel AE, Sabin ND, et al. Conformal radiation therapy for pediatric ependymoma, chemotherapy for incompletely resected ependymoma, and observation for completely resected, supratentorial ependymoma. *J Clin Oncol* 2019;37:974–983.
43. Ay H, Gungor L, Arsava EM, et al. A score to predict early risk of recurrence after ischemic stroke. *Neurology* 2010;74:128–135.
44. Virani SS, Alonso A, Benjamin EJ, et al. Heart disease and stroke statistics—2020 update. *Circulation* 2020;141:e139–e596.
45. Harnarine-Singh D, Hyde JB. Postnatal growth of the arterial net in the human cerebral pia mater. *Nature* 1970;225:86–87.
46. Otto KB, Lieser W. The capillaries of various parts of the human brain in the fetal period and during the first years of life. *Acta Anat (Basel)* 1970;77:25–36.
47. Breier G, Albrecht U, Sterrer S, et al. Expression of vascular endothelial growth factor during embryonic angiogenesis and endothelial cell differentiation. *Development* 1992;114:521–532.
48. Breier G, Risau W. The role of vascular endothelial growth factor in blood vessel formation. *Trends Cell Biol* 1996;6:454–456.
49. Mancuso MR, Kuhnert F, Kuo CJ. Developmental angiogenesis of the central nervous system. *Lymphat Res Biol* 2008;6:173–180.
50. Pearce WJ. Fetal cerebrovascular maturation: Effects of hypoxia. *Semin Pediatr Neurol* 2018;28:17–28.
51. Bitzer M, Topka H. Progressive cerebral occlusive disease after radiation therapy. *Stroke* 1995;26:131–136.
52. Mori K, Takeuchi J, Ishikawa M, et al. Occlusive arteriopathy and brain tumor. *J Neurosurg* 1978;49:22–35.
53. Campen CJ, Kranick SM, Kasner SE, et al. Cranial irradiation increase risk of stroke in pediatric brain tumor survivors. *Stroke* 2012;43:3035–3040.
54. Hall EJ, Giaccia AJ. Clinical response of normal tissues. *Radiobiol Radiol* 2006;6:333–337.
55. Hong J-H, Chiang C-S, Campbell IL, et al. Induction of acute phase gene expression by brain irradiation. *Int J Radiat Oncol Biol Phys* 1995;33:619–626.
56. Kim JH, Brown SL, Jenrow KA, et al. Mechanisms of radiation-induced brain toxicity and implications for future clinical trials. *J Neurooncol* 2008;87:279–286.
57. Kortmann R-D, Timmermann B, Taylor RE, et al. Current and future strategies in radiotherapy of childhood low-grade glioma of the brain. *Strahlenther Onkol* 2003;179:509–520.
58. Li Y-Q, Ballinger JR, Nordal RA, et al. Hypoxia in radiation-induced blood-spinal cord barrier breakdown. *Cancer Res* 2001;61:3348–3354.
59. Ljubimova NV, Levitman MK, Plotnikova ED, et al. Endothelial cell population dynamics in rat brain after local irradiation. *Br J Radiol* 1991;64:934–940.
60. Reinhold HS, Calvo W, Hopewell JW, et al. Development of blood vessel-related radiation damage in the fimbria of the central nervous system. *Int J Radiat Oncol Biol Phys* 1990;18:37–42.
61. Toussaint L, Peters S, Mikkelsen R, et al. Delineation atlas of the Circle of Willis and the large intracranial arteries for evaluation of doses to

- neurovascular structures in pediatric brain tumor patients treated with radiation therapy. *Acta Oncologica* 2021;60:1392–1398.
62. Moher D, Liberati A, Tetzlaff J, et al. Preferred reporting items for systematic reviews and meta-analyses: The PRISMA statement. *PLoS Med* 2009;6:e1000097.
 63. Moiseenko V, Marks LB, Grimm J, et al. A primer on dose-response data modeling in radiation therapy. *Int J Radiat Oncol Biol Phys* 2021;110:11–20.
 64. Mahadevan A, Moningi S, Grimm J, et al. Maximizing tumor control and limiting complications with stereotactic body radiation therapy for pancreatic cancer. *Int J Radiat Oncol Biol Phys* 2021;110:206–216.
 65. Miften M, Vinogradskiy Y, Moiseenko V, et al. Radiation dose-volume effects for liver SBRT. *Int J Radiat Oncol Biol Phys* 2021;110:196–205.
 66. Truelsen T, Begg S, Mathers C. The global burden of cerebrovascular disease. World Health Organization 2006. Available at: https://www.who.int/healthinfo/statistics/bod_cerebrovasculariseasestroke.pdf. Accessed January 27, 2021.
 67. Fullerton HJ, Wu YW, Sidney S, et al. Risk of recurrent childhood arterial ischemic stroke in a population-based cohort: The importance of cerebrovascular imaging. *Pediatrics* 2007;119:495–501.
 68. Ganesan V, Prengler M, McShane MA, et al. Investigation of risk factors in children with arterial ischemic stroke. *Ann Neurol* 2003;53:167–173.
 69. Hills NK, Johnston SC, Sidney S, et al. Recent trauma and acute infection as risk factors for childhood arterial ischemic stroke. *Ann Neurol* 2012;72:850–858.
 70. Lanthier S, Carmant L, David M, et al. Stroke in children: The coexistence of multiple risk factors predicts poor outcome. *Neurology* 2000;54:371–378.
 71. Mackay MT, Wiznitzer M, Benedict SL, et al. Arterial ischemic stroke risk factors: The International Pediatric Stroke study. *Ann Neurol* 2011;69:130–140.
 72. Hall MD, Bradley JA, Rotondo RL, et al. Risk of radiation vasculopathy and stroke in pediatric patients treated with proton therapy for brain and skull base tumors. *Int J Radiat Oncol Biol Phys* 2018;101:854–859.
 73. Strenger V, Sovinz P, Lackner H, et al. Intracerebral cavernous hemangioma after cranial irradiation in childhood. Incidence and risk factors. *Strahlenther Onkol* 2008;184:276–280.
 74. van Dijk IW, van der Pal HJ, van Os RM, et al. Risk of symptomatic stroke after radiation therapy for childhood cancer: A long-term follow-up cohort analysis. *Int J Radiat Oncol Biol Phys* 2016;96:597–605.
 75. Freund D, Zhang R, Sanders M, et al. Predictive risk of radiation induced cerebral necrosis in pediatric brain cancer patients after VMAT versus proton therapy. *Cancers (Basel)* 2015;7:617–630.
 76. Abolfath R, Peeler CR, Newpower M, et al. A model for relative biological effectiveness of therapeutic proton beams based on a global fit of cell survival data. *Sci Rep* 2017;7:8340.